Paper for AIAA Joint Propulsion Conference, July 27-29, 2015, Orlando, Florida

Generalized Fluid System Simulation Program (GFSSP) – Version 6

By

Alok Majumdar, Andre LeClair, Ric Moore
NASA/Marshall Space Flight Center
&
Paul Schallhorn
NASA/Kennedy Space Center

Abstract

The Generalized Fluid System Simulation Program (GFSSP) is a finite-volume based general-purpose computer program for analyzing steady state and time-dependent flow rates, pressures, temperatures, and concentrations in a complex flow network. The program is capable of modeling real fluids with phase changes, compressibility, mixture thermodynamics, conjugate heat transfer between solid and fluid, fluid transients, pumps, compressors, flow control valves and external body forces such as gravity and centrifugal. The thermo-fluid system to be analyzed is discretized into nodes, branches, and conductors. The scalar properties such as pressure, temperature, and concentrations are calculated at nodes. Mass flow rates and heat transfer rates are computed in branches and conductors. The graphical user interface allows users to build their models using the 'point, drag, and click' method; the users can also run their models and post-process the results in the same environment. The integrated fluid library supplies thermodynamic and thermo-physical properties of 36 fluids, and 24 different resistance/source options are provided for modeling momentum sources or sinks in the branches. Users can introduce new physics, non-linear and time-dependent boundary conditions through user-subroutine.

1. Introduction

The need for a generalized computer program for thermo-fluid analysis in a flow network has been felt for a long time in Aerospace Industries. Designers of thermo-fluid systems often need to know pressures, temperatures, flowrates, concentrations, and heat transfer rates at different parts of a flow circuit for steady state or transient conditions. Such applications occur in propulsion systems for tank pressurization, internal flow analysis of rocket engine turbo-pumps, chilldown of cryogenic tanks and transfer lines and many other applications of gas-liquid systems involving fluid transients and conjugate heat and mass transfer. Computer resource requirements to perform time-dependent three-dimensional Navier-Stokes Computational Fluid Dynamic (CFD) analysis of such systems are prohibitive and therefore are not practical. A possible recourse is to construct a fluid network consisting of a group of flow branches such as pipes and ducts that are joined together at a number of nodes. They can range from simple systems consisting of a few nodes and branches to very complex networks containing many flow branches simulating valves, orifices, bends, pumps and turbines. In the analysis of existing or proposed networks, node pressures, temperatures and concentrations at the

system boundaries are usually known. The problem is to determine all internal nodal pressures, temperatures, concentrations and branch flow rates. Such schemes are known as Network Flow Analysis methods and they use largely empirical information to model fluid friction and heat transfer.

The oldest method for systematically solving a problem consisting of steady flow in a pipe network is the Hardy Cross method [1]. The Hardy Cross method works well for hand calculation but experiences slow convergence for large circuit, The network analysis method has been widely used in thermal analysis codes (SINDA/G [2] and SINDA/FLUINT [3]) using an electric analog. The partial differential equation of heat conduction is discretized into finite difference form expressing temperature of a node in terms of temperatures of neighboring nodes and ambient nodes. The set of finite difference equations are solved to calculate temperature of the solid nodes and heat fluxes between the nodes. GFSSP [4] uses a "pressure-based" finite volume method [5] as the foundation of its numerical scheme.

This paper provides a brief overview of GFSSP's network definition, data structure, mathematical formulation, thermodynamic property program and program structure and describes additional capabilities of version 6. The paper also describes several validation and verification effort.

2. GFSSP Overview

2.1 Network Definition

A fluid network using fluid and solid nodes. The fluid circuit is constructed with boundary nodes, internal nodes and branches (Figure 1) while the solid circuit is constructed with solid nodes, ambient nodes and conductors. The solid and fluid nodes are connected with solid-fluid conductors. Users must specify conditions, such as pressure, temperature and concentration of species at the boundary nodes. These variables are calculated at the internal nodes by solving conservation equations of mass, energy and species in conjunction with the thermodynamic equation of state. Each internal node is a control volume where there are inflow and outflow of mass, energy and species at the boundaries of the control volume. The internal node also has resident mass, energy and concentration. The momentum conservation equation is expressed in flowrates and is solved in branches. At the solid node, the energy conservation equation for solid is solved to compute temperature of the solid node. Figure 1 shows a schematic and GFSSP flow circuit of a counter-flow heat exchanger. Hot nitrogen gas is flowing through a pipe, colder nitrogen is flowing counter to the hot stream in the annulus pipe and heat transfer occurs through metal tubes. The problem considered is to calculate flowrates and temperature distributions in both streams.

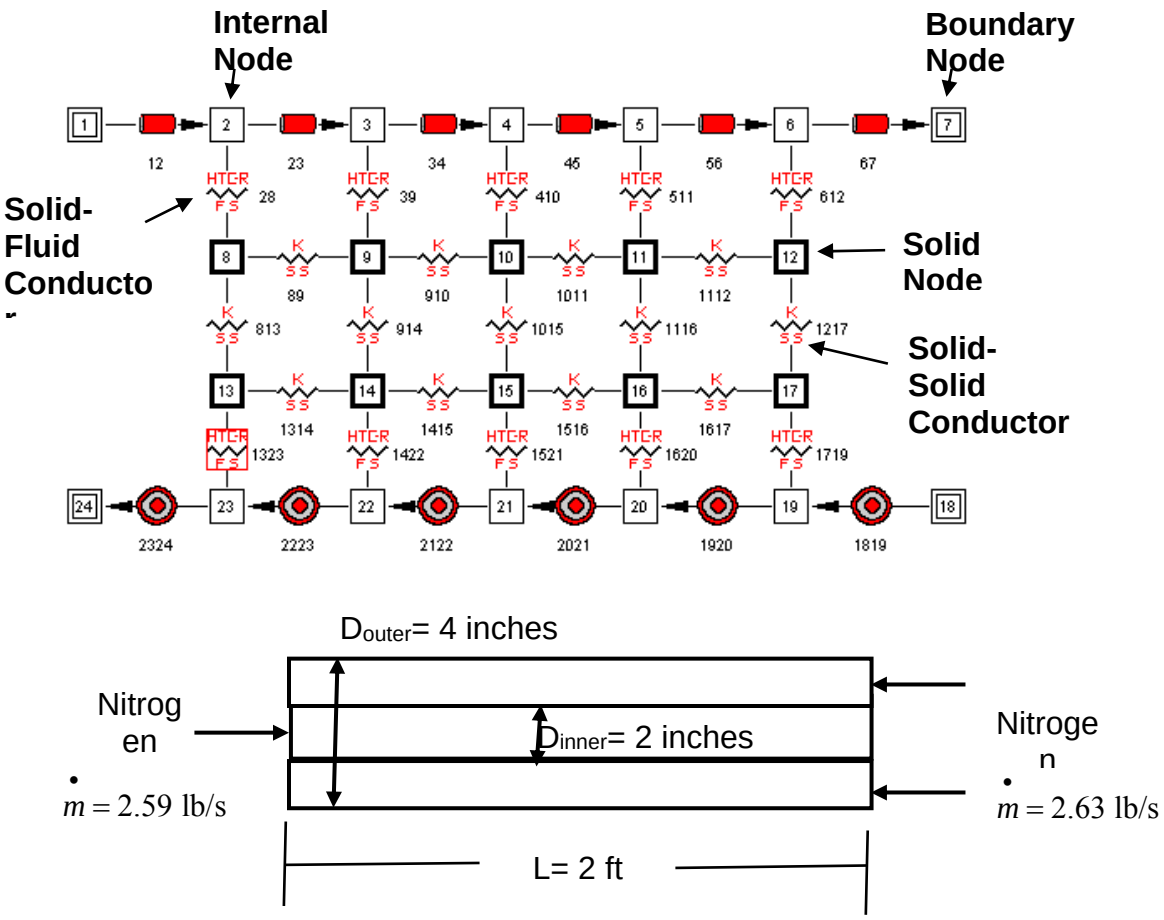

Figure 1 – A Typical Flow Network consists of Fluid Node, Solid Node, Flow Branches and Conductors

2.2 Data Structure

GFSSP has a unique data structure (Figure 2) that allows constructing all possible arrangements of a flow network with no limit on the number of elements. The elements of a flow network are boundary nodes, internal nodes and branches. For conjugate heat transfer problems, there are three additional elements, solid node, ambient node and conductor. The relationship between a fluid node and a branch as well as a solid node and conductor is defined by a set of relational geometric properties. For example the relational geometric properties of a node are number and name of branches connected to it. With the help of these properties, it is possible to define any structure of the network as it progresses through every junction of the network. The positive or negative flow direction is also defined locally. Unlike structured co-ordinate system, there is no global definition of flow direction and origin. The development of a flow network can start from any point and can proceed in any direction.

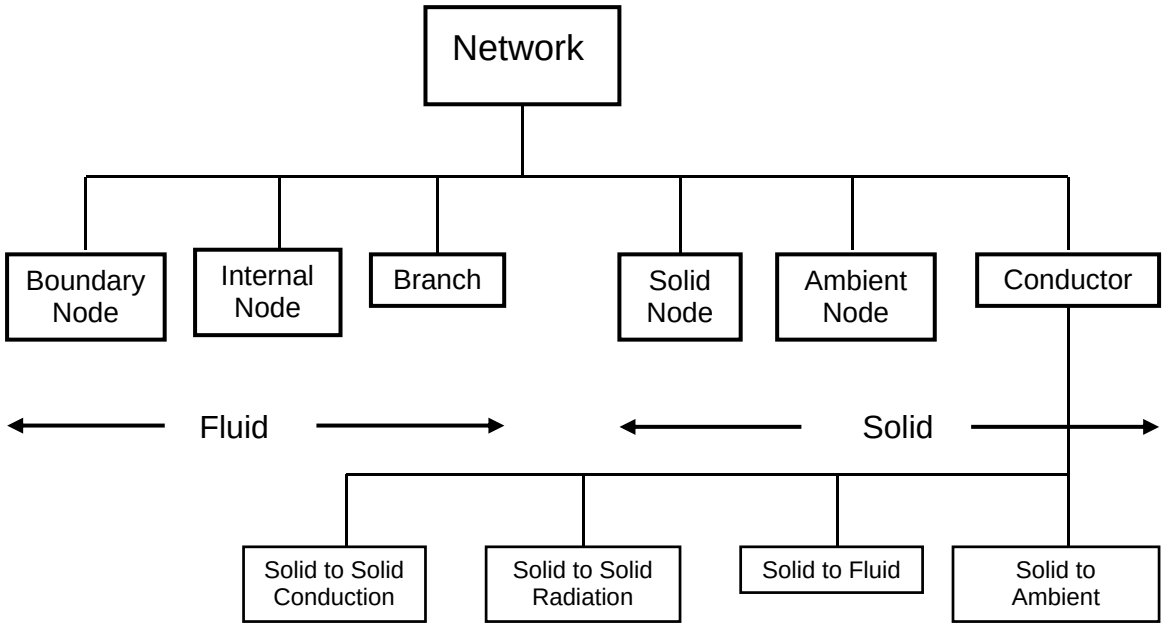

Figure 2 – Data Structure of the Fluid-Solid Network has Six Major Elements

2.2 Mathematical Formulation

GFSSP solves the conservation equations of mass and momentum in internal nodes and branches to calculate fluid properties. It also solves for energy conservation equations to calculate temperatures of solid nodes. Table 1 shows the mathematical closure that describes the unknown variables and the available equations to solve the variables. Pressure, temperature, species concentration and resident mass in a control volume are calculated at the internal nodes whereas the flowrate is calculated at the branch. The equations are coupled and non-linear. Therefore, they are solved by an iterative numerical scheme. GFSSP employs a unique numerical scheme known as Simultaneous Adjustment with Successive Substitution (SASS) which is a combination of Newton-Raphson and Successive Substitution methods. The mass and momentum conservation equations and the equation of state are solved by the Newton-Raphson method while the conservation of energy and species are solved by the successive substitution method.

Table 1 Mathematical Closure

Unknown Variables	Available Equations to Solve
1. Pressure	**1. Mass Conservation Equation**
2. Flowrate	**2. Momentum Conservation Equation**
3. Fluid Temperature	**3. Energy Conservation Equation of Fluid**
4. Solid Temperature	**4. Energy Conservation Equation of Solid**
5. Species Concentrations	**5. Conservation Equations for Species**
6. Fluid Mass (Unsteady Flow)	**6. Thermodynamic Equation of State**

2.3 Fluid Properties

GFSSP is linked with two thermodynamic property programs, GASP & WASP [6, 7] and GASPAK [8] that provide thermodynamic and thermo-physical properties of selected fluids. Both programs cover a range of pressure and temperature that allows fluid properties to be evaluated for liquid, liquid-vapor (saturation) and vapor region. GASP and WASP provide properties of twelve fluids (Table 2). GASPAK includes a library of thirty six fluids (Table 3).

Table 2 - Fluids Available in GASP & WASP

Index	Fluid	Index	Fluid
1	HELIUM	7	ARGON
2	METHANE	8	CARBON DIOXIDE
3	NEON	9	FLUORINE
4	NITROGEN	10	HYDROGEN
5	CARBON MONOXIDE	11	WATER
6	OXYGEN	12	RP-1

Table 3 – Fluids Available in GASPAK

Index	Fluid	Index	Fluid
1	HELIUM	19	KRYPTON
2	METHANE	20	PROPANE
3	NEON	21	XENON
4	NITROGEN	22	R-11
5	CO	23	R12
6	OXYGEN	24	R22
7	ARGON	25	R32
8	CO_2	26	R123
9	PARAHYDROGEN	27	R124
10	HYDROGEN	28	R125
11	WATER	29	R134A
12	RP-1	30	R152A
13	ISOBUTANE	31	NITROGEN TRIFLUORIDE
14	BUTANE	32	AMMONIA
15	DEUTERIUM	33	IDEAL GAS
16	ETHANE	34	HYDROGEN PEROXIDE
17	ETHYLENE	35	AIR
18	HYDROGEN SULFIDE		

2.4 Program Structure

GFSSP has three major parts (Figure 3). The first part is the Graphical User Interface, VTASC (Visual Thermofluid Analyzer of Systems and Components). VTASC allows users to create a flow circuit by a 'point and click' paradigm. It creates the GFSSP input file after the completion of the model building process. It can also create a customized GFSSP executable by compiling and linking User Subroutines with the solver module of the code. Users can run GFSSP from VTASC and post process the results in the same environment. The second major part of the program is the Solver and Property Module. This is the heart of the program that reads the input data file, generates the required conservation equations for all internal nodes and branches with the help of thermodynamic property data. It also interfaces with User Subroutines to receive any specific inputs from users. Finally, it creates output files for VTASC to read and display results. The User Subroutine is the third major part of the program. This consists of several blank subroutines that are called by the Solver Module. These subroutines allow the users to incorporate any new physical model, resistance option, fluid etc. in the model.

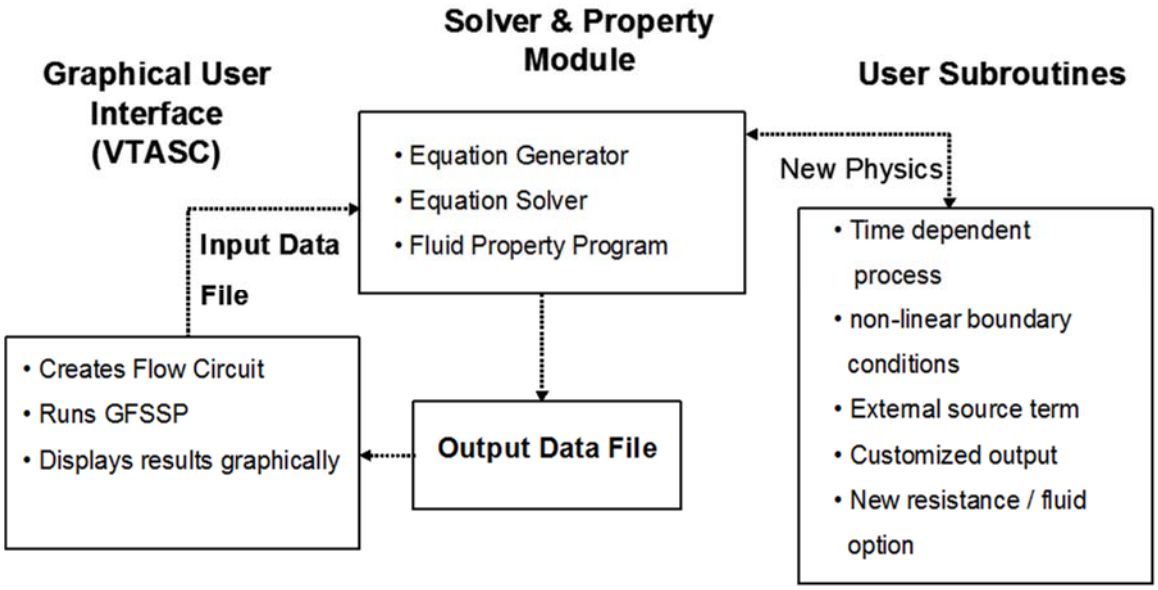

Figure 3 - GFSSP's Program Structure showing the interaction of three major modules

2.5 Resistance Option

In network flow analysis code, flow resistances are modeled by empirical laws. These empirical laws have been incorporated to model flow resistances for pipe flow, orifices, valves and various pipe fittings. GFSSP models these flow resistances in the momentum conservation equation as a friction term. There are twenty-four different resistance options available to users to choose from. There is also a provision for introducing a new resistance option through user subroutines. The available resistance options are shown in Table 4.

2.6 Graphical User Interface

GFSSP's Graphical User Interface provides the users a platform to build and run their models. It also allows post-processing of results. The network flow circuit is first built using three basic elements: boundary node, internal node and branch. Then the properties of the individual elements are assigned. Users are also required to define global options of the model that includes input/output files, fluid specification and any special options such as rotation, heat exchanger etc. During execution of the program, a run manager window opens up and users can monitor the progress of the numerical solution. On the completion of the run, it allows users to visualize the results in tabular form for steady-state solutions and in graphical form for unsteady solutions. It also provides an interface to activate and import data to the plotting program, WINPLOT [9] for post processing.

Table 4 - Resistance Options in GFSSP

Option	Type of Resistance	Input Parameters	Option	Type of Resistance	Input Parameters
1	Pipe Flow	L (in), D (in), ε/D	13	Common Fittings and Valves (Two K Method)	D (in), K_1, K_2
2	Flow Through Restriction	C_L, A (in^2)	14	Pump Characteristics[1]	A_0, B_0, C_0, A (in^2)
3	Non-circular Duct	a (in), b (in)	15	Pump Power	P (hp), η, A (in^2)
4	Pipe with Entrance and Exit Loss	L (in), D (in), ε/D, K_i, K_e	16	Valve with Given C_v	C_v , A
5	Thin, Sharp Orifice	D_1 (in), D_2 (in)	17	Joule-Thompson Device	L_{ohm}, V_f, k_v, A
6	Thick orifice	L (in), D_1 (in), D_2 (in)	18	Control Valve	See Example 12 data file
7	Square Reduction	D_1 (in), D_2 (in)	19	User Defined	A (in^2)
8	Square Expansion	D_1 (in), D_2 (in)	20	Heat Exchanger Core	A_f (in^2), A_s(in^2), A_c (in^2), L(in), K_c, K_e
9	Rotating Annular Duct	L (in), r_o (in), r_i (in), N (rpm)	21	Parallel Tube	L (in), D (in), ε/D, n
10	Rotating Radial Duct	L (in), D (in), N (rpm)	22	Compressible Orifice	C_L, A (in^2)
11	Labyrinth Seal	r_i (in), c (in), m (in), n, α	23	Labyrinth Seal, Egli Correlation	r_i (in), c (in), m (in), n, α
12	Flow Between Parallel Plates	r_i (in), c (in), L (in)	24	Fixed Flow	Flow (lb_m/s), A (in_2)

[1] Pump characteristics are expressed as $\Delta p = A_0 + B_0 \dot{m} + C_0 \dot{m}^2$

Δp - Pressure rise, lbf/ft^2

$\dot{m}$ - Flow rate, lbm/sec

2.7 Example Problems

Several example problems have been included to aid users to become familiar with different options of the code. The example problems also provide the verification and validation of the code by comparing code's predictions with analytical solution and experimental data. The example problems are:

(1) Simulation of a flow system consisting of a pump, valve, and pipe line.
(2) Simulation of a water distribution network.
(3) Simulation of compressible flow in a converging-diverging nozzle.
(4) Simulation of the mixing of combustion gases and a cold gas stream.
(5) Simulation of a flow system involving a heat exchanger.
(6) Radial flow on a rotating radial disk.
(7) Flow in a long-bearing squeeze film damper.
(8) Simulation of the blowdown of a pressurized tank.
(9) A reciprocating piston-cylinder.
(10) Pressurization of a propellant tank.
(11) Power balancing of a turbopump assembly.
(12) Helium pressurization of LOX and RP-1 propellant tanks.
(13) Steady state and transient conduction through a circular rod, with convection.
(14) Chilldown of a short cryogenic pipe line.
(15) Simulation of fluid transient following sudden valve closure.
(16) Simulation of pressure regulator downstream of a pressurized tank.
(17) Simulation of flow regulator downstream of a pressurized tank.
(18) Subsonic Fanno flow.
(19) Subsonic Rayleigh flow.
(20) Modeling of closed cycle liquid metal (lithium) loop with heat exchanger to heat helium gas.
(21) Internal flow in a turbopump.
(22) Simulation of a fluid network with fixed flow rate option.
(23) Helium-assisted, buoyancy-driven flow in a vertical pipe carrying LOX with ambient heat leak.
(24) Simulation of relief valve in a pressurized tank.
(25) Two-dimensional recirculating flow in a driven cavity.
(26) Fluid transients in pipes due to sudden opening of valve.
(27) Boiling water reactor.
(28) No-vent tank chill and fill model.
(29) Self-pressurization of a cryogenic propellant tank due to boil-off.
(30) Modeling solid propellant ballistic with GFSSP.

The Tables (5a & 5b) show the particular features of each example problem. For example, “Conjugate Heat Transfer” option has been used in Examples 13, 14, 23, 26 and 29.

Table 5a

Table 14a. Use of various options in example problems—examples 1–15.

Feature	Example														
	1	2	3	4	5	6	7	8	9	10	11	12	13	14	15
Conjugate heat transfer													13	14	
Constant property		2					7								
Cyclic boundary															
Fixed mass flow															
Flow regulator															
Gravity	1														
Heat exchanger					5						11				
Ideal gas								8							
Long inertia			3			6						12			
Fluid mixture				4						10		12			
Model import															
Moving boundary							7		9						
Multilayer insulation															
Multidimensional flow															
Noncircular duct							7								
Phase change														14	
Pressurization (tank)										10		12			
Pressure regulator															
Pressure relief valve															
Pump	1											12			
Solid rocket motor															
Turbopump											11				
Turbopump—internal flow															
Unsteady								8	9	10		12		14	15
User fluid															
User subroutine										10		12			
Valve O/C															15
Variable geometry									9						
Fluid transient (water hammer)															15

Table 5b

Table 14b. Use of various options in example problems—examples 16–30.

Feature	Example														
	16	17	18	19	20	21	22	23	24	25	26	27	28	29	30
Conjugate heat transfer								23					28	29	
Constant property										25					
Cyclic boundary					20										
Fixed mass flow							22						28		
Flow regulator		17													
Gravity								23				27	28	29	
Heat exchanger					20										
Ideal gas	16	17													30
Long inertia			18	19								27			30
Fluid mixture								23							
Model import								23							
Moving boundary											26*				
Multilayer insulation														29	
Multidimensional flow										25					
Noncircular duct															
Phase change												27	28	29	
Pressurization (tank)														29	
Pressure regulator	16														
Pressure relief valve									24						
Pump															
Solid rocket motor															30
Turbopump															
Turbopump—internal flow						21									
Unsteady	16	17					22	23	24		26		28	29	30
User fluid					20							27			
User subroutine			18	19	20						26		28	29	30
Valve O/C											26				
Variable geometry											26*				
Fluid transient (water hammer)											26				

*Variable geometry and moving boundary handled by User Subroutine.

3. Additional Capabilities of Version 6

The additional capabilities of Version 6 include improved modeling of fluid mixtures, multi-dimensional flow capability in a system level flow network model, extension of the thermo-dynamic property package, extension of the pressure and flow regulator option, and inclusion of the relief valve and fixed flowrate options.

3.1 Mixture modeling

The mixture modeling capability in earlier version of GFSSP did not allow phase change for any component of the mixture. This limitation was due to the fact that the energy conservation equation was expressed as a product of specific heat and temperature instead of enthalpy. In many liquid propulsion applications, phase change in mixture is a common occurrence when cryogenic propellants mix with inert gas such as helium or nitrogen. This limitation was removed in Version 6 by introducing an additional option where the energy equation of each species was expressed in terms of enthalpy. This option allows change of phase for any component of the mixture.

3.2 Multi-dimensional flow capability

Version 6 allows the user to model multi-dimensional flow in a fluid network. Network modeling usually applies to a system where a one-dimensional momentum equation is sufficient to characterize the flow. However, in some situations, such as a stratified cryogenic tank, the one-dimensional flow assumption is not realistic. Multi-dimensional flow modeling in a system level code will eliminate the need to integrate with a CFD code which has not yet been proved to be a practical solution. Multi-dimensional flow modeling in a system level code is a viable alternative to address such a need. Multi-dimensional capability in GFSSP has been verified by comparing its predictions with classical numerical fluid dynamics problems such as flow in a driven cavity.

3.3 Improvements and Extension in Thermodynamic Property Routines

There has been significant improvement and extension of the thermodynamic property routines in Version 6. The thermodynamic property routines have been rewritten to introduce universal property call subroutines. In this process the fluid property code has been reduced by nearly 1000 lines. With the introduction of the new property call routines, user subroutines can make property calls during any stage of the computation.

The user supplied fluid property table has been extended to include an optional saturation table. It may be noted that earlier version of GFSSP did not have the capability to model phase change with user supplied fluid property tables. Utility programs have been

developed to generate user supplied thermodynamic property tables from tables generated by REFPROP [10] and are included in the GFSSP installation package.

3.4 Extension of pressure and flow regulator option

A marching algorithm [11] for modeling pressure and flow regulator has been introduced in Version 6. The earlier option of iterative algorithm is still available. The marching algorithm is more economic and allows the use of multiple regulators in a given flow circuit.

3.5 Inclusion of relief valve and fixed flowrate option

Version 6 has also the capability of modeling relief valve and a fixed flowrate option. It may be recalled that GFSSP's mathematical formulation requires pressures to be specified at boundary nodes and flowrates are calculated by solving the momentum conservation equation. In this version the user can specify a given flowrate in a branch connected with a boundary node. This option is available for both steady and unsteady flow.

4. Validation & Verification

Several code validation efforts were completed during the development of Version 6. The applications considered for code validation include fluid transient, chilldown of cryogenic transfer line, self-pressurization of cryogenic tank, and no vent chill and fill of cryogenic tank.

4.1 Two-dimensional recirculating flow in a square cavity

In this example, two-dimensional recirculating flow in a square cavity [12] has been modeled using GFSSP's multi-dimensional flow calculation capability. In a square cavity the flow is induced by shear interaction at the top wall as shown in Figure 4. The length of each wall is 12 inches. The density of the fluid is assumed constant at 1.00 lb_m/ft^3, and the viscosity of the fluid is assumed to be 1.00 $lb_m/(ft \cdot sec)$. The bottom and side walls are fixed. The top wall is moving to the right at constant speed of 100 ft/sec. The corresponding Reynolds number for this situation is Re = 100.

The GFSSP model (Figure 5) of the driven cavity consists of 50 nodes (49 of which are internal) and 84 branches. System model is shown in Figure 5a. The expanded component (square cavity) is shown in Figure 5b.

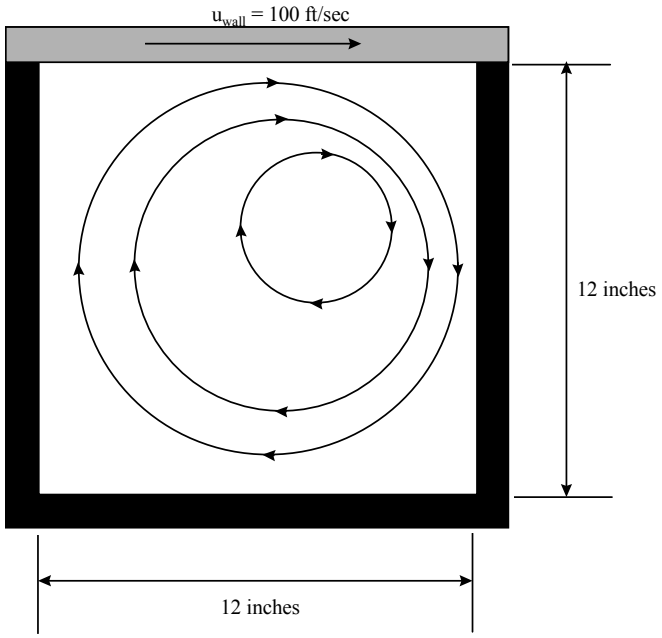

Figure 4- Flow in a Shear Driven Square Cavity

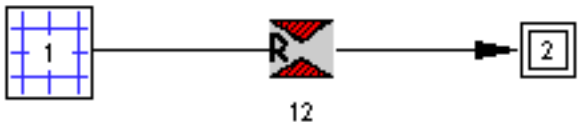

(a) System Network with expandable grid (Element 1)

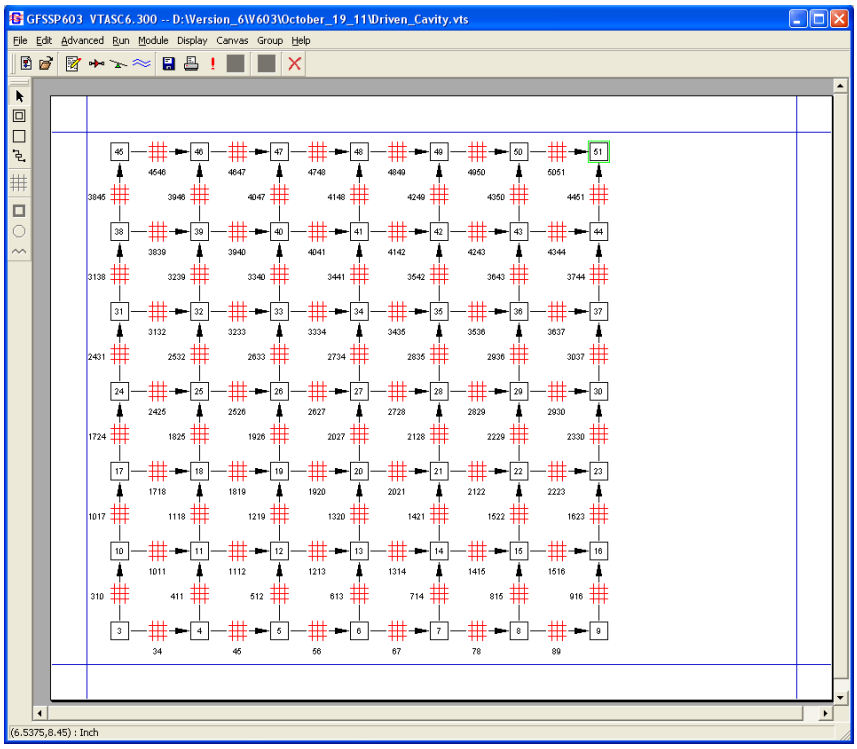

(b) Expanded two-dimensional Cartesian grid of Element 1

Figure 5- Two-dimensional Cartesian grid generation in VTASC

Figure 6 shows a comparison between the benchmark numerical solution and GFSSP 7x7 node model velocity profiles along a vertical plane at the horizontal midpoint. As can be seen in Figure 6, the results of this crude GFSSP model compare very favorably with the benchmark numerical solution of Burggraf [13].

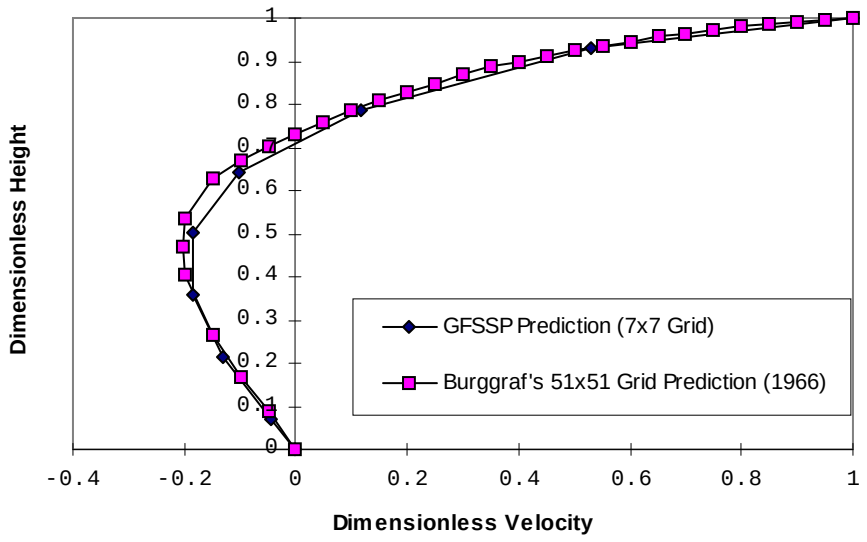

Figure 6. Shear Driven Square Cavity Centerline Velocity Distribution

The predicted velocity field and pressure contours are shown in Figure 7. The recirculating flow pattern and stagnation of flow near the top right corner are clearly shown in the figure. The predicted stream traces from calculated velocity field is shown in Figure 8.

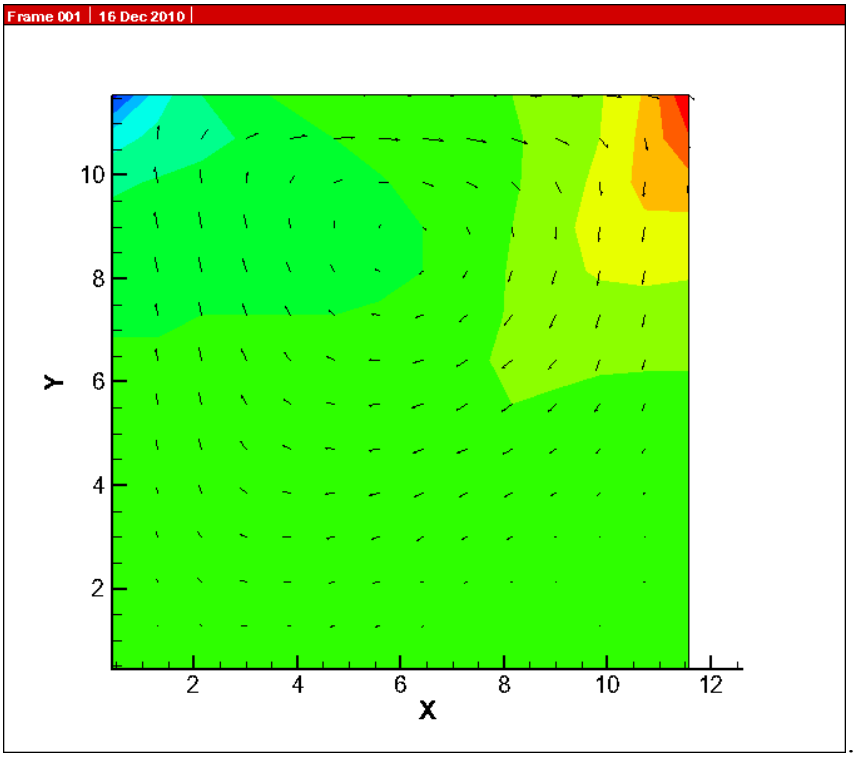

Figure 7 - Predicted Velocity Field and Pressure Contours

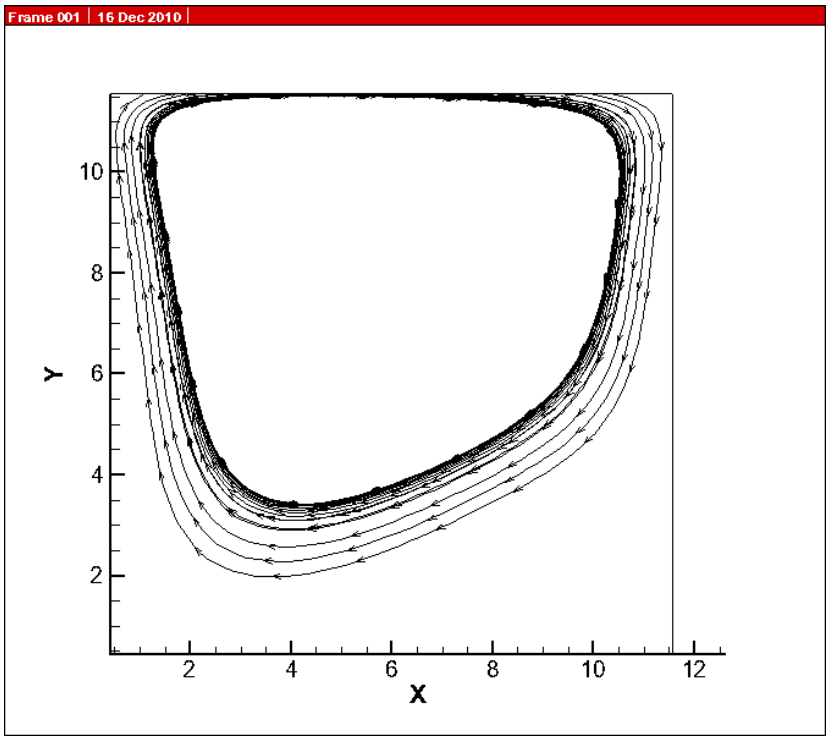

Figure 8 - Predicted Stream Traces in the Driven Cavity

4.2 Fluid Transient

This example deals with water hammer in a pipe with entrapped air. GFSSP results are validated against experimental data available in the literature [14]. A long pipe of diameter 1.025 inches is attached to a reservoir of water at one end and closed at the other end with some entrapped air in the other end. A ball valve separates the water from the air as shown in Figure 9 below. The ball valve is closed until about 0.15 second, and then gradually opens to 100% at about 0.4 second. This example has been set up according to the experimental study done by Lee et al[14]. The two most important controlling parameters for this problem are the reservoir pressure (p_R) and the fractional air length present in the pipe as compared to the total pipe length ($\alpha_g = L_g/L_T$). The initial length for the water volume in the pipe (L_l) is fixed to 20 ft, and initial length of air column in the pipe (L_g) varies from a low of 1.23 ft to 16.23 ft, the value of α ranging from 0.0579 to 0.448 respectively. The ratio of reservoir pressure to the initial pressure of the entrapped air ($P_R = p_R/p_{atm}$) varies in the range of 2 to 7, i.e. the reservoir pressure (p_R) range being 29.4 psi to 102.9 psi. The objective of this study is to predict the transient pressure at different points along the length of the pipe.

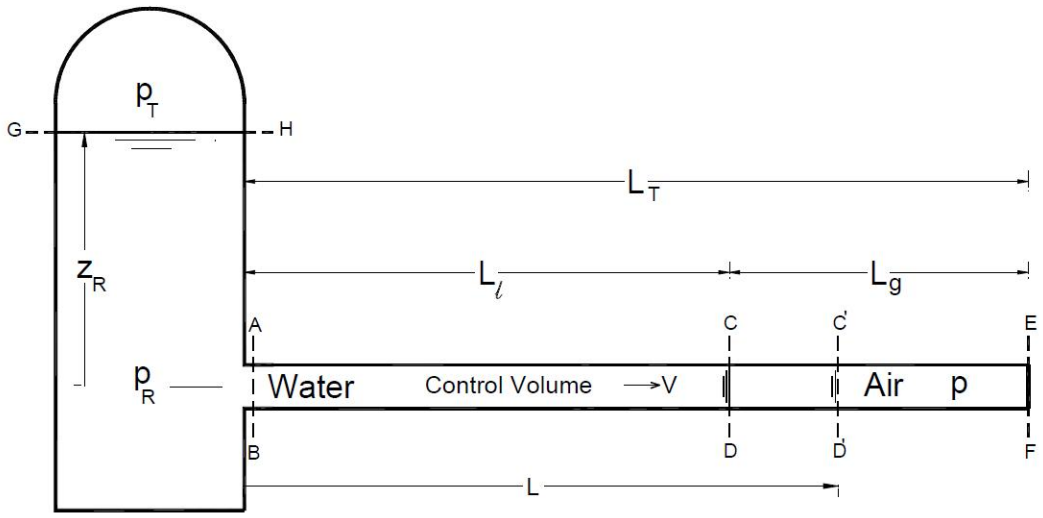

Figure 229. Schematic of the Water Pipe with Entrapped Air

The GFSSP model to represent the flow of water in the pipe is shown in Figure 10. The pipe sector of length 20 feet (only the water column) is divided into ten uniform pipe segments and one restriction separating twelve nodes. Boundary Node 1 represents the tank (reservoir). A user subroutine interfaces Node 12 to an unseen pseudo control volume containing air only. The pseudo control volume has a fixed mass of air, but the volume changes as it is pressurized owing to the fluctuation of pressure at node 12. Thereby the volume of node 12 changes as the volume of the imaginary control volume changes. The volume change in node 12 is computed by a volume balance between the volume of water and the volume of the entrapped air. The total volume ($V_{tot} = V_{air} + V_{12}$) remains constant, and must be equal to the initial total volume (since the pipe is closed at the other end).

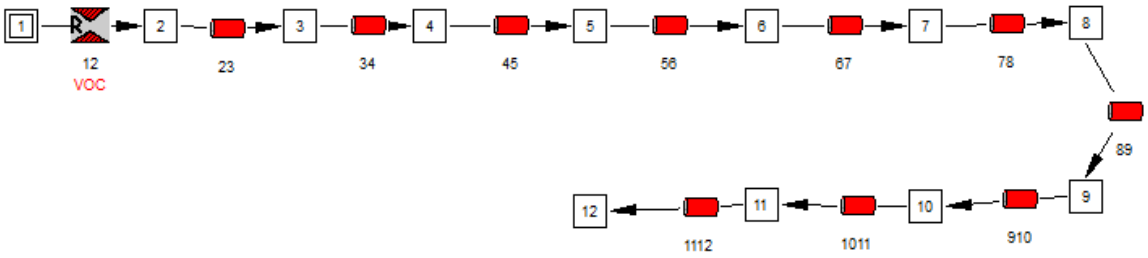

Figure 10. GFSSP Model of Sudden Valve Opening Experiment of Lee & Martin[54]

For the numerical solution a time step of 0.01 s has been used. The operating conditions are: PR = 7, and $\alpha_g = 0.45$). Figure 11 compares GFSSP's predicted pressure at node 12 with that of the experimental data points of Lee and Martin. The predicted results compared very well, and even though the peak pressure amplitude differs by about 7%, the frequencies of pressure oscillations matched very well.

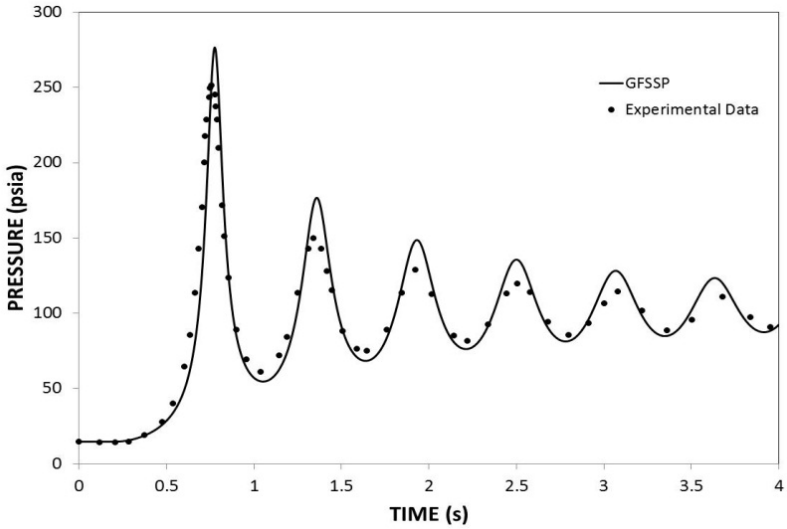

Figure 11. Comparison of GFSSP and Experimental Data

A Fast Fourier Transform (Figure 12) has been conducted in the numerical model to predict the different modal frequencies of the pressure transient and also compared with the experimental data. More details of this example problem is available in Reference [15].

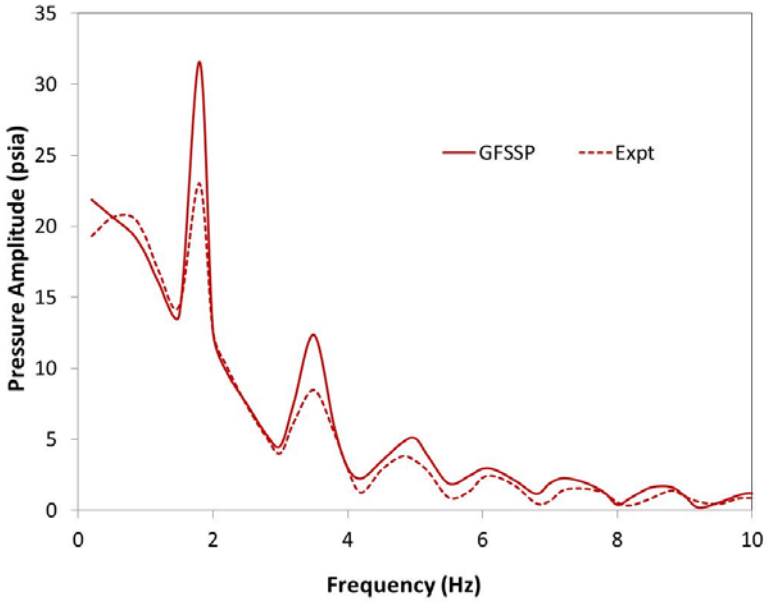

Figure 12. Fast Fourier Transform for Modal Frequencies

4.3 Chilldown of Cryogenic Transfer Line

For this example, the chilldown of cryogenic pipeline to validate GFSSP's transient conjugate heat transfer capability has been selected. In the 1960s the National Bureau of Standards (NBS) conducted a series of chilldown experiments on a cryogenic transfer line [16]. The test setup (Figure 13) is a vacuum-jacketed 200 foot long copper pipe of 5/8 inch inner diameter. A pressurized 80 gallon dewar feeds liquid hydrogen into the pipe that is initially at ambient temperature. The wall temperature is measured at four thermocouple stations at distances of 20, 80, 141, and 198 feet from the inlet.
When the fluid touches the relatively warm pipe walls, heat transfer causes the liquid cryogen to boil and the pipe wall temperature to decrease. Eventually the pipe chills down to the liquid temperature, and the liquid front gradually travels further down the pipeline. At the outlet of the pipeline, vapor exits to the atmosphere.

The NBS experiments were conducted with liquid hydrogen (LH2) and liquid nitrogen (LN2) at various driving pressures with saturated and sub-cooled fluid. This example problem models one of the tests with an inlet boundary of saturated LH2 at 74.97 psia and -411 °F.

Figure 14 shows the GFSSP model of the chilldown experiment. The 200 ft pipe line has been discretized into 30 pipe segments, each with 80 inches of pipe length. There are 31 fluid nodes, each fluid node is connected with solid nodes. The total mass is distributed to 31 solid nodes. The fluid and solid nodes are connected by solid to fluid conductors. The solid nodes are connected by solid to solid conductors. The boundary nodes 1 and 33 represent the inlet dewar and ambient outlet respectively.

The solid nodes are connected to the fluid nodes by Fluid-to-Solid Conductors, which model convection from the fluid to the pipe wall. The built-in Miropolskii correlation [17] is used to calculate the convection coefficient for the two-phase flow. Because the pipe is vacuum-jacketed, heat transfer between the pipe walls and the ambient is assumed negligible.

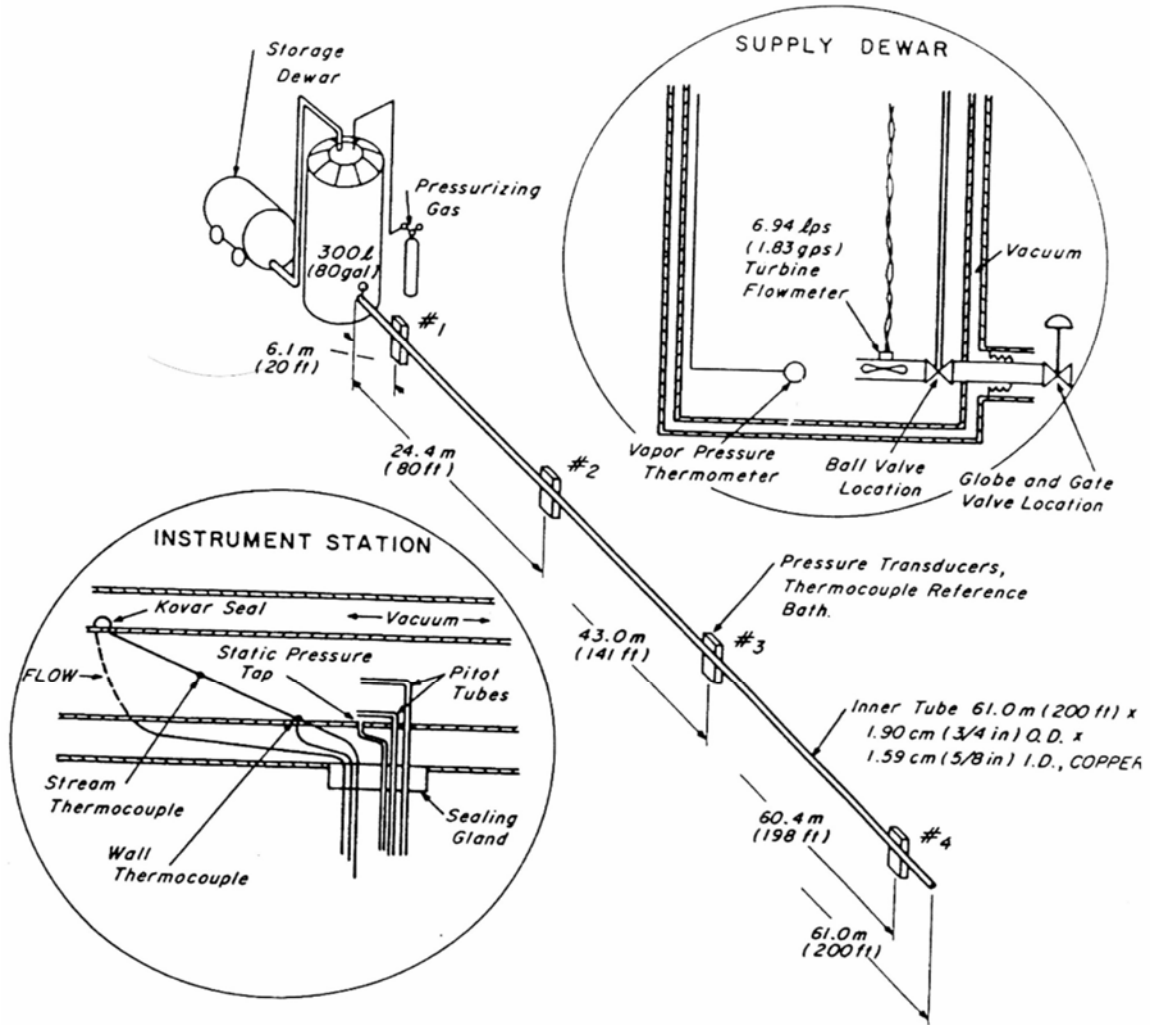

Figure 13. NBS Test Set-up of Cryogenic Transfer Line

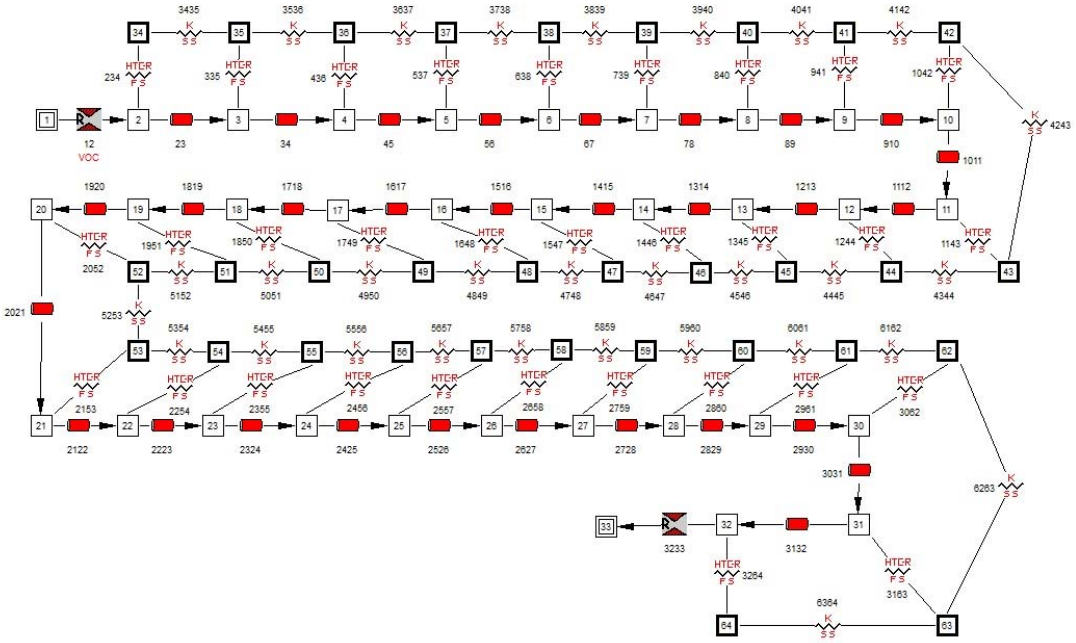

Figure 14. GFSSP Model of the Cryogenic Pipeline

Figure 15 shows the comparison between predicted and measured temperature at 4 measuring stations are shown in this slide. The predictions and measurements compare reasonably well. In general measurements show more rapid chilldown than predictions. This discrepancy can be attributed to the deficiency of heat transfer correlation that does not account for other boiling regimes such as nucleate and transition.

The comparison of measured and predicted chilldown time of the transfer line at different driving pressures for both liquid hydrogen and nitrogen is shown Table 6. Chilldown time decreases with increasing pressure primarily due to higher flowrate at higher pressure. Sub-cooling helps reduce chilldown time. Generally, predicted chilldown time is slightly higher than measured data. Discrepancy between the prediction and measurements can be attributed to the inaccuracy in heat transfer coefficient correlation as discussed in the previous paragraph. More details about this validation appear in Reference 18.

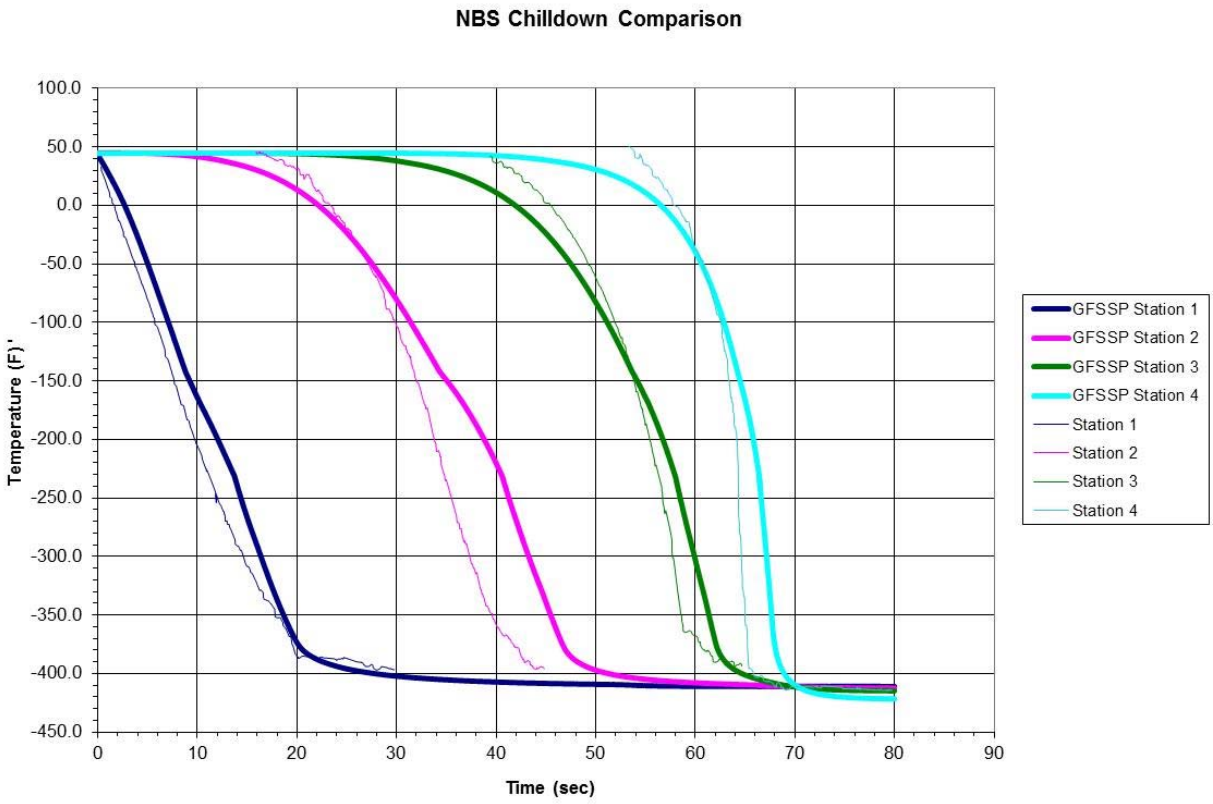

Figure 15. GFSSP's Predicted Solid Temperatures (°F) Compared to Measurements

Table 6 Measured and Predicted Chilldown Time for NBS Test Setup

Saturated LH_2 chilldown time for various driving pressures

Driving Pressure (psia)	Saturation Temperature (°F)	Experimental Chilldown Time (s)	Predicted Chilldown Time (s)
74.97	–411.06	68	70
86.73	–409.08	62	69
111.72	–406.4	42	50
161.72	–402.13	30	33

Subcooled LH_2 chilldown time for various driving pressures. LH_2 is subcooled at –424.57 ºF

Driving Pressure (psia)	Experimental Chilldown Time (s)	Predicted Chilldown Time (s)
36.75	148	150
61.74	75	80
86.73	62	60
111.72	41	45
136.72	32	35
161.7	28	30

Saturated LN_2 chilldown time for various driving pressures

Driving Pressure (psia)	Saturation Temperature (°F)	Experimental Chilldown Time (s)	Predicted Chilldown Time (s)
61.74	–294.09	165	185
74.97	–289.71	150	160
86.73	–286.24	130	140

Subcooled LN_2 chilldown time for various driving pressures. LN_2 is subcooled at –322.87 ºF

Driving Pressure (psia)	Experimental Chilldown Time (s)	Predicted Chilldown Time (s)
36.75	222	250
49.97	170	175
61.74	129	140
74.97	100	100
86.73	85	90

4.4 Self-pressurization of cryogenic tank

The purpose of this example is to demonstrate the simulation of self-pressurization of a Liquid Hydrogen Tank performed under the Multi-Purpose Hydrogen Test Bed (MHTB) program [19]. The purpose of the MHTB program is to test a Thermodynamic Vent System (TVS) to reduce boil-off in a Cryogenic Propellant Tank for long term storage of propellant in space as shown schematically in Figure 245.

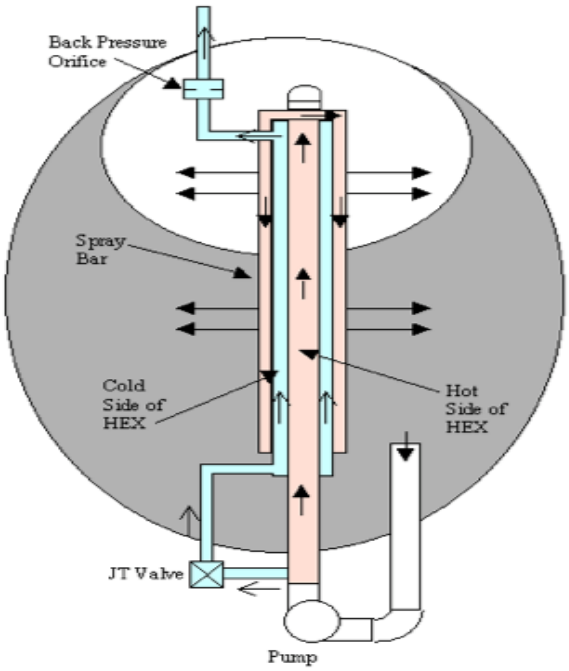

Figure 16. Thermodynamic Vent System in MHTB Tank

The MHTB 5083 aluminum tank is cylindrical in shape with a height and diameter of 10 feet and elliptic domes in both ends as shown in Figure 17. It has an internal volume of 639 ft^3 and surface area of 379 ft^2. Initially the tank is allowed to self- pressurize due to boil-off and by not allowing the vapor to vent. Once the pressure reaches the maximum allowable pressure, liquid hydrogen is introduced into the tank through the spray bar. The pressure starts falling due to heat transfer, and when the pressure reaches the minimum allowable pressure, the spray is stopped and the tank is allowed to self-pressurize and thus TVS cycle continues. The purpose of the GFSSP model is to simulate the initial self-pressurization when ullage pressure rises from the initial tank pressure to the upper bound pressure when the spray starts. The GFSSP model results were then compared with the test data. A 50% Fill Level case was modeled to simulate the self-pressurization test.

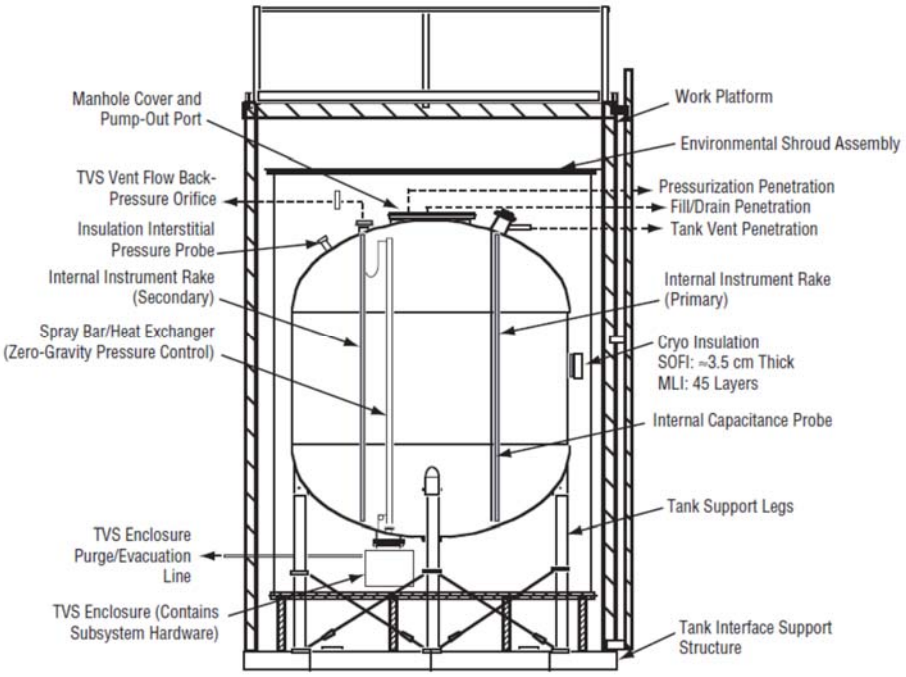

Figure 17. MHTB Test Tank and Supporting Hardware Schematic

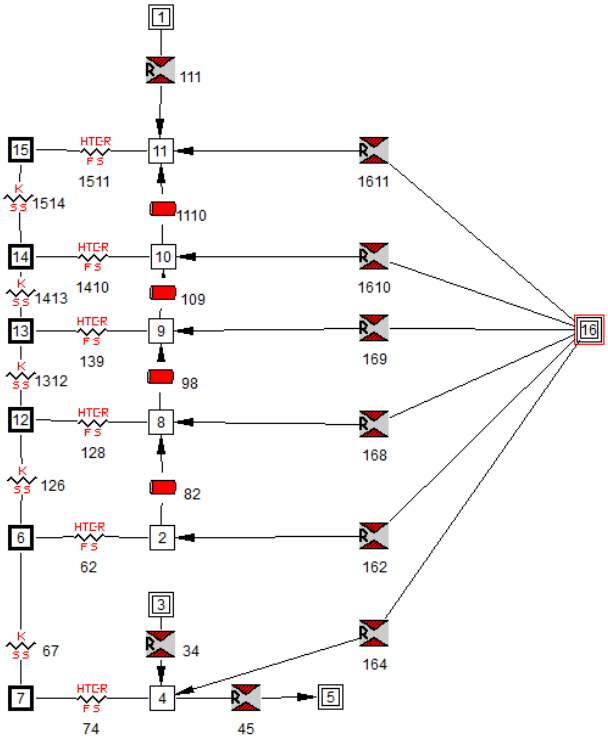

Figure 18. GFSSP Model of MHTB Test Tank

Figure 18 shows the GFSSP model of self-pressurization in the MHTB Tank at the 50% fill level. Node 4 represents liquid hydrogen; Nodes 2, 8, 9, 10, and 11 represent the ullage at different fill levels. Node 3 is a pseudo-boundary node separating liquid hydrogen from

vapor hydrogen in the ullage space. Branches 45, 164, 162, 168, 169, 1610 and 1611 are for introducing liquid hydrogen into the tank through the TVS spray bar. These branches are currently inactive during self-pressurization of the tank. Node 7, 6, 12, 13, 14 and 15 are solid nodes representing the aluminum tank wall. Solid Node 7 is connected with liquid hydrogen stored in Fluid Node 4. In this model, heat leak through insulation is calculated in the User Subroutine and applied in the solid nodes as a source term.

In this model a User Subroutine was used a) to model evaporative mass transfer at the liquid-vapor interface, b) to calculate the heat transfer coefficient between the wall and the fluid nodes, and c) to calculate heat transfer through the MLI blankets. The details of the modeling appear in reference 20.

Figure 19 shows the comparison between GFSSP predictions (in green and blue) and the MHTB Test Data (in orange). GFSSP predictions of pressure are shown for a Degradation Factor of 1 and 2.8. The Degradation Factor is used to multiply Equation 3.5.7 to represent the degradation of performance of the MLI. It is observed that a Degradation Factor of 2.8 matches the test data well.

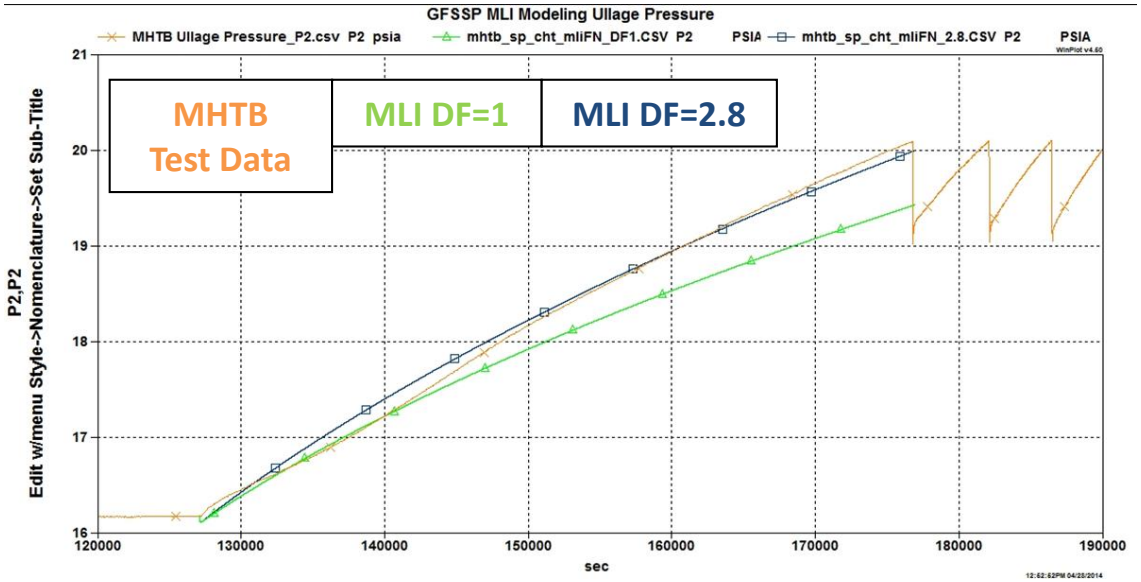

Figure 19. Application Results for MHTB Self Pressurization Model

4.5 No vent chill and fill of cryogenic tank

The purpose of this example is to demonstrate the simulation of the no-vent chill and fill method of chilling and filling a cryogenic tank. The practice of tank chilldown in micro-gravity environment is quite different than tank chilldown on the ground. On the ground, under normal gravity, a vent valve on top of the tank can be kept open to vent the vapor generated during the chilling process. The tank pressure can be kept close to atmospheric pressure while the tank is chilling down. In a micro-gravity environment, due to the absence of stratification, such practice may result in dumping a large amount of precious propellant overboard. The intent of the no-vent chill and fill method is to minimize the loss of propellant during chilldown of a propellant tank in a micro-gravity environment. The no-vent chill and fill method consists of a repeated cyclic process of charge, hold, and vent.

During the charge cycle, a small quantity of liquid cryogen is injected into the evacuated tank. Some type of spray nozzle is usually used to break the incoming liquid into droplets. Initially, the liquid flashes due to the low tank pressure, and then the remaining liquid droplets evaporate as they contact warm hydrogen vapor or the tank wall. During the hold period, the circulating flow pattern induced from the spray nozzles provides convective heat transfer from cold vapor to the tank wall. The primary mode of heat transfer during the hold is convection. At the completion of the hold period, the pressure has risen considerably and the tank is ready to be vented. Since venting occurs as an isentropic blow-down, some additional cooling may be recovered by stage-wise venting. The key parameters of this method are (1) charge magnitude, (2) spray system selection, (3) mass flow rate, (4) hold duration, (5) acceleration environment, (6) desired tank wall temperature, and (7) maximum operating pressure. A reliable and inexpensive mathematical model will help designers to perform a large amount of calculations to optimize the key parameters. A GFSSP model was developed to simulate chilldown of the LH2 tank at the K-site Test Facility [21] and numerical predictions were compared with test data.

The test set-up at the K-site Test Facility, shown in Figure 20, consists of a test tank, spray system, test tank valves, instrumentation, and the vacuum chamber.

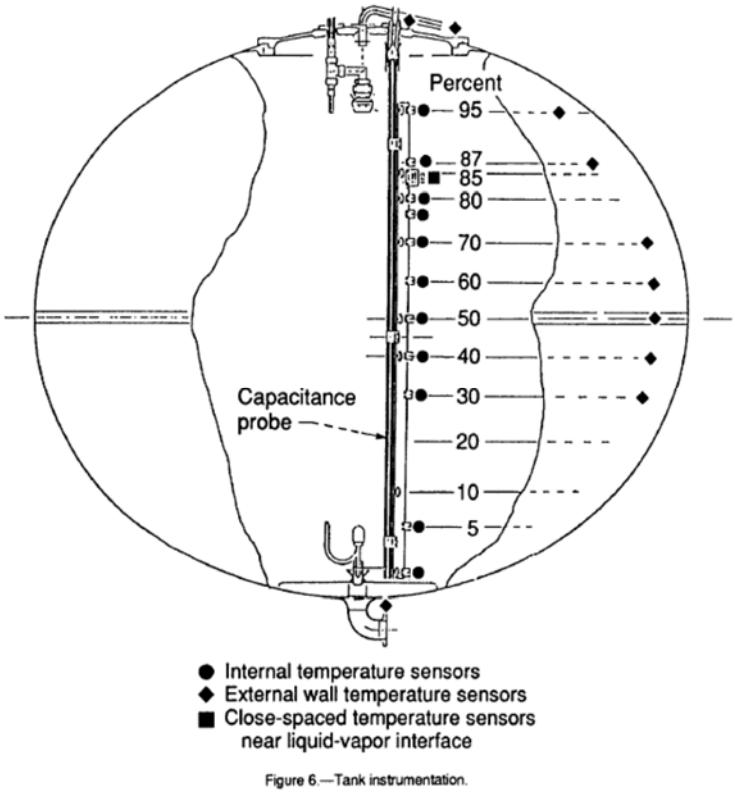

Figure 6.—Tank instrumentation.

Figure 20. K-Site Test Set-Up for No-Vent Fill Experiment

The test tank selected was ellipsoidal with an 87 inch major diameter and a 1.2 to 1 major to minor axis ratio. The two ends are joined by a short 1.5 inch cylindrical section. The tank is made of 2219 aluminum chemically milled to a nominal thickness of 0.087 inches. Thicker sections exist where they were required for manufacturing (mainly weld lands). The tank has a 28.35 inch access flange on the top. The tank weighs 329.25 pounds, and the tank's volume is 175 ft^3. The tank was originally designed for a maximum operating pressure of 80 psia. Prior to the start of testing the tank was re-qualified by pneumatic test for a maximum operating pressure of 50 psia. The tank is covered with a blanket of 34 layers of multi-layer insulation (MLI) made with double aluminized Mylar and silk net spacers, and is supported by 12 fiberglass epoxy struts. The test environment ambient temperature was uniform and maintained at 530R ± 1R by an electrically heated shroud located outside the tank and inside the vacuum chamber.

A nine node tank model (Figure 21) was developed to model this experiment. The tank was discretized into nine nodes and eight branches. Each fluid node was connected to a corresponding solid node. The total flowrate was equally distributed into 9 branches with fixed flowrate option.

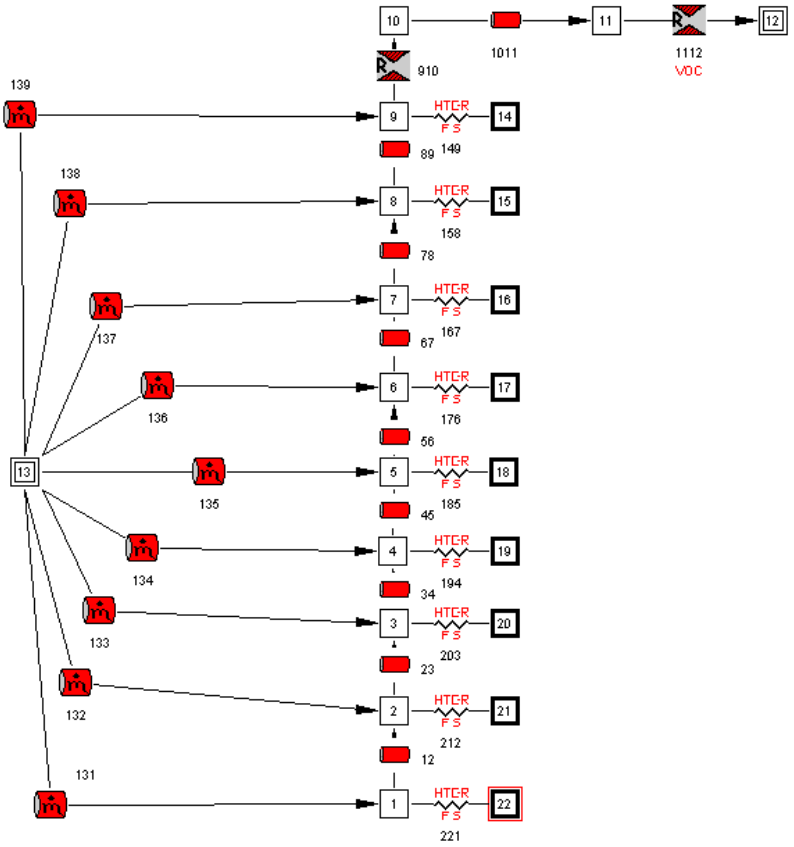

Figure 21. GFSSP Nine Node Tank Model

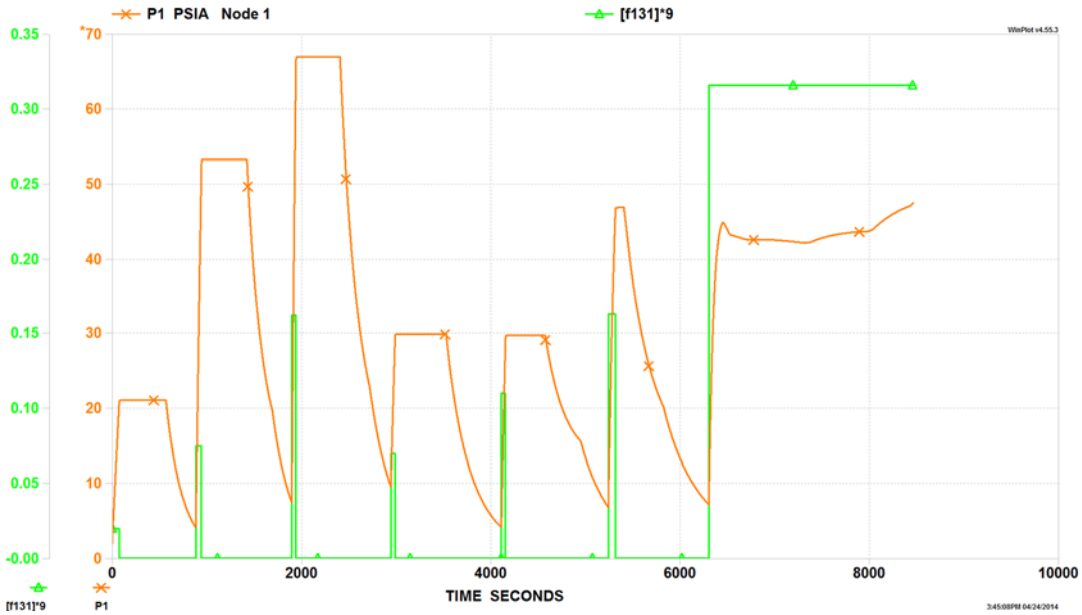

Figure 22. Specified Inlet Flowrate (green) and Predicted Pressure (Orange) History

Inlet flowrate into the tank and predicted pressure are shown in Figure 22. There are five short pulses of liquid hydrogen flow into the tank. After each pulse, there is a period of

no flow into the tank. During this period, the tank holds the propellant with vent valve closed for the tank to reach thermal equilibrium with cold vapor. Pressure rises almost instantaneously because of liquid turning into vapor with large increase in specific volume. The pressure continues to increase at a lower rate due to heat transfer from wall during this hold period. The hold period is followed by venting causing pressure to drop rapidly. After shutting the vent valve, the next pulse of inlet flow occurs. After five pulses, a constant inlet flow was maintained to fill the tank. Once the continuous filling starts, pressure initially drops due to some condensation of vapor in the tank. Once the tank is getting nearly filled, pressure rises due to the compression of vapor in the ullage space.

Figure 22 shows the predicted mass history of hydrogen during the operation. There is very little hydrogen during the chilling process because of venting. The total amount of propellant vapor vented during this period is 32.5 lbs. This number compares well (within 1.5%) with measured propellant loss during the test.

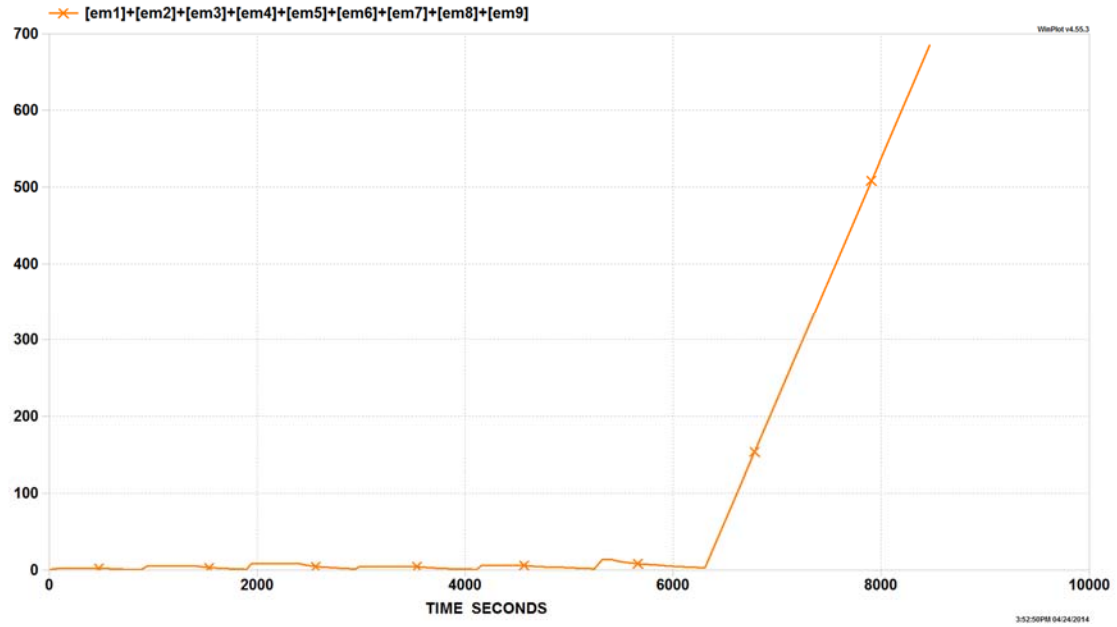

Figure 22. Predicted Hydrogen Mass History in the Tank

Temperatures were measured during the test. The upper and lower bound of measured temperature history is shown in Figure 23. GFSSP model results for single and nine node are also shown to compare the predicted and test data. For nine node model, the centerline temperature is plotted.

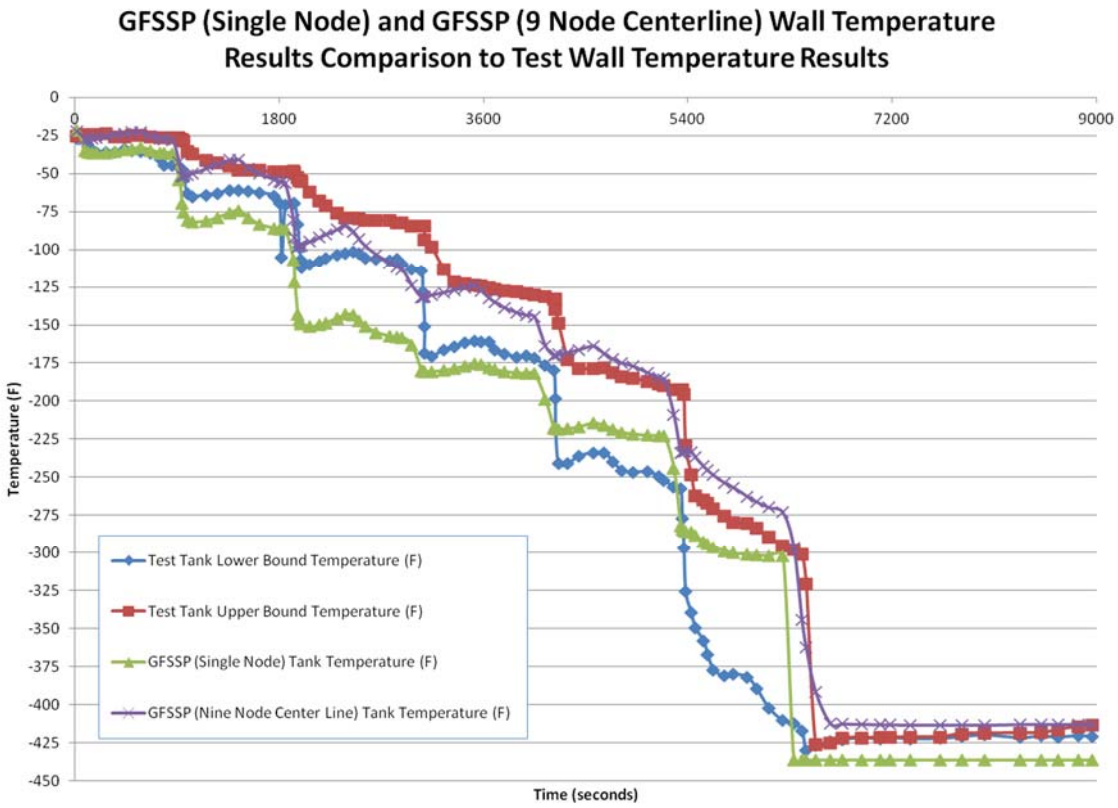

Figure 23. Comparison of predicted and measured wall temperature during no-vent fill for the K-site test tank.

5. Conclusions

This paper explains the basic features of NASA's Generalized Fluid System Simulation Program (GFSSP) and describes the additional capabilities of Version 6. Several numerical models are presented to illustrate code's application in simulating Fluid Transient and Cryogenic Fluid Management (CFM) applications such as chilldown of cryogenic transfer line, no-vent chill and fill of cryogenic tank and self-pressurization of cryogenic tank. Numerical results are compared with test data.

Acknowledgements

GFSSP development was supported by National Institute of Rocket Propulsion (NIRPS) at Marshall Space Flight Center, Launch Service Program at Kennedy Space Center and e CRYO program at Glenn Research Center. The authors wish to acknowledge the service of Technology Transfer Office and Publication Office at MSFC for distribution of GFSSP and preparation of this manuscript.

References

1. Streeter, V.L., "Fluid Mechanics", 3rd Edition, McGraw-Hill, 1962.
2. SINDA/G Thermal Analyzer, Network Analysis Inc, http://www.sinda.com
3. SINDA/FLUINT, Heat Transfer and Fluid Flow Design and Analysis Software, C&R Technologies, http://www.crtech.com/sinda.html
4. A.K. Majumdar, A.C. LeClair, R. Moore, P.A. Schallhorn, Generalized Fluid System Simulation Program, Version 6.0, NASA/TM—2013–217492 (October 2013) <https://gfssp.msfc.nasa.gov>.
5. Patankar, S. V., "Numerical Heat Transfer and Fluid Flow", Hemisphere Publishing Corp., Washington, D. C., 1980.
6. Hendricks, R. C., Baron, A. K., and Peller, I. C., "GASP - A Computer Code for Calculating the Thermodynamic and Transport Properties for Ten Fluids: Parahydrogen, Helium, Neon, Methane, Nitrogen, Carbon Monoxide, Oxygen, Fluorine, Argon, and Carbon Dioxide", NASA TN D-7808, February, 1975.
7. Hendricks, R. C., Peller, I. C., and Baron, A. K., "WASP - A Flexible Fortran IV Computer Code for Calculating Water and Steam Properties", NASA TN D-7391, November, 1973.
8. Cryodata Inc., "User's Guide to GASPAK, Version 3.20", November 1994.
9. "WINPLOT version 4.3" Users Manual, NASA/Marshall Space Flight Center
10. Eric W. Lemmon, Marcia L. Huber, Mark O. McLinden, "NIST Reference Fluid Thermodynamic and Transport Properties— REFPROP, Version 8.0, User's Guide, http://www.nist.gov/srd/upload/REFPROP8.PDF
11. Schallhorn, Paul and Hass, Neal, "Forward Looking Pressure Regulator Algorithm for Improved Modeling Performance Within the Generalized Fluid System Simulation Program", 40th AIAA/ASME/SAE/ASEE Joint Propulsion Conference and Exhibit, Fort Lauderdale, Florida, July 11-14, 2004, AIAA-2004-3667.
12. Schallhorn, Paul and Majumdar, Alok, "Implementation of Finite Volume based Navier Stokes Algorithm within General Purpose Flow Network Code", 50th AIAA Aerospace Sciences Meeting held on 9-12 January, 2012 in Nashville, Tennessee.
13. Burggraf, O.R.: "Analytical and Numerical Studies of the Structure of Steady Separated Flows", Journal of Fluid Mechanics, Vol. 24, part 1, pp. 113-151, 1966.
14. N.H. Lee, C.S Martin, Experimental and analytical investigation of entrapped air in a horizontal pipe, *Proceedings of the 3rd ASME/JSME Joint Fluids Engineering Conference*, ASME, New York, NY (July 18–23, 1999) pp. 1–8.
15. Bandyopadhyay, A. and Majumdar, A., "Network Flow Simulation of Fluid Transients in Rocket Propulsion System" *Journal of Propulsion and Power*, October, 2014
16. Brennan, J. A., Brentari, E. G., Smith, R. V., and Steward, W. G., "Cooldown of Cryogenic Transfer Lines, An Experimental Report," National Bureau of Standards Report 9264, November 1966.
17. Cross, M.; Majumdar, A.; Bennett, J.; and Malla, R.: "Modeling of Chill Down in Cryogenic Transfer Lines," *J. Spacecraft Rockets*, Vol. 39, No. 2, pp. 284–289, 2002.
18. Majumdar, Alok and Ravindran, S.S., "Numerical Modeling of Conjugate Heat Transfer in Fluid Network", *Journal of Propulsion and Power,* Volume 27(3), pp.620-630, 2011.

19. Martin, J.J.; and Hastings L.J.: “Large-Scale Liquid Hydrogen Testing of a Variable Density Multilayer Insulation With a Foam Substrate,” NASA/TM—2001–211089, NASA Marshall Space Flight Center, Huntsville, AL, 88 pp., June 2001.
20. Majumdar, Alok; Valenzuela, Juan; LeClair, Andre and Moder, Jeff, “Numerical Modeling of Self-Pressurization and Pressure Control by Thermodynamic Vent System in a Cryogenic Tank”, to be presented at Space Cryogenics Workshop, June 24-26, 2015, Phoenix, Arizona.
21. Chato, David & Sanabria, Rafael, “Review and Test of Chilldown Methods for Space-Based Cryogenic Tanks”, NASA Technical Memorandum 104458, AIAA-91-1843.
22. Majumdar, Alok, “No vent tank fill and transfer line chilldown analysis by Generalized Fluid System Simulation Program”, TFAWS 2013, July 29-August 2, 2013, KSC, Florida